Modeling of Transient Currents in Polyethylene Terephtalate

N. Saidi-Amroun[a]; S. Berdous[a]; M. Saidi[a]; M. Bendaoud[a]

[a] Physics Faculty, Material Physics Laboratory, University of Science and Technology (USTHB), Algiers, Algeria

PLEASE SCROLL DOWN FOR ARTICLE

Taylor & Francis
Taylor & Francis Group

Modeling of Transient Currents in Polyethylene Terephtalate

N. Saidi-Amroun, S. Berdous, M. Saidi, and M. Bendaoud
Physics Faculty, Material Physics Laboratory, University of Science and
Technology (USTHB), Algiers, Algeria

Abstract: The effect of temperature on transient electrical charging current in gold metallized polyethylene terephthalate (PET), which is a polymer of particular interest in electrical applications, was analyzed and compared with the results of previous work on aluminum metallized PET. Charging and discharging currents were measured with electrical fields ranging from 24×10^6 to 56×10^6 V/m and temperatures between $40°$ and $140°$C. A model based on space charge formation was proposed. Simulated current showed good agreement with experimental current. This model allowed us to calculate space charge distribution and internal field.

Keywords: Charging current peak; Electrical conduction; Polyethylene terephtalate

INTRODUCTION

Polyethylene terephthalate (PET) is often used as a dielectric in high-performance foil capacitors (class-E insulators). Therefore, there is much interest in the electrical and dielectric properties of this material from the technological point of view. Although a number of studies have been made on transient current in organic polymers, there are many problems

not yet well understood. The charging current after DC voltage application is known to decay with time until steady-state current is achieved. Removing the external voltage causes a discharging current flow in the opposite direction, usually equal to the charging current reduced by the steady-state current. The time-dependent current, $J(t)$, follows the empirical Curie-Von Schweidler law[1] t^{-m}, where t is a time after the application of the field and m is a constant often observed to be close to unity.

In this study, the temperature dependence of the transient current in polyethylene terephthalate has been investigated. The anomalous charging current peak was observed. Several works have reported the existence of this peak with different polymers, like polyethylene (PE),[2–6] polyethylene terephthalate (PET),[7,8] polypropylene (PP),[9] polyvinylidene fluoride (PVDF),[10–11] and polyethylene naphthalate (PEN).[12,13] Several models have been proposed to explain the anomalous current.

In a previous work,[14] a model was used that explains and reproduces experimental features of transient current. In this article, a numerical model, consisting of injection current and dipolar current, is proposed. It is parameterized so as to fit a set of experimental measurements of current in two kinds of electrode metals at different temperatures. The aim is to show temperature effect and electrode nature effect on experimental and simulated current and, consequently, to deduce the impact of the variation of the chosen parameters.

EXPERIMENTAL PROCEDURE

The PET sample, 25×10^{-6} m thick, was supplied by the firm Rhône Poulenc. The film was prepared with gold or aluminum evaporated electrodes, 1 cm in diameter, on both sides of the sample.

The experimental apparatus used in our investigations and the measurement procedure are described elsewhere.[12,14] The PET was exposed to a DC voltage at a constant temperature, and the charging current was measured for period of up to 1×10^4 s.

EXPERIMENTAL RESULTS

Figure 1 shows charging current density $J(t)$ characteristics obtained in a temperature range of 70°–100°C for an applied field of 56×10^6 V/m. At the temperature of $T = 70^{\circ}$C, the current decreases monotonously with time over several orders of magnitude following the Curie law, then reaches a steady value within a few hours. While at temperatures of 90° and 100°C, the current at first decreases, after this, it increases, and finally, it decreases again until it reaches a steady-state value, showing
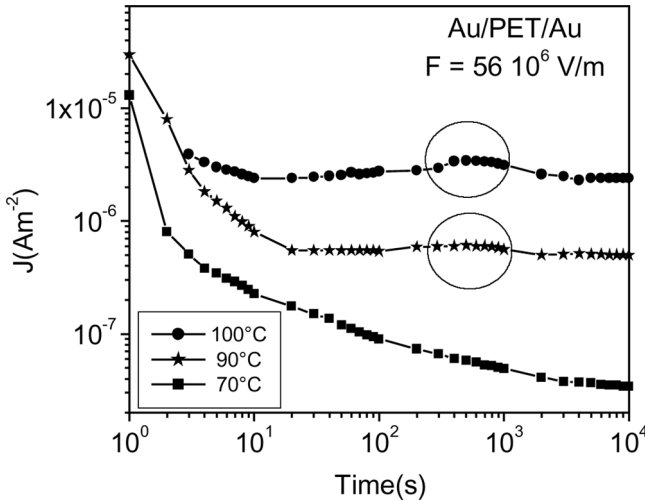
Figure 1. Current-time characteristics of PET at various temperatures.

a peak at 700 and 500 s respectively. This current is the so-called "anomalous charge current." In this case, the current can be described by the Curie law only at the initial stage of charging; after that it deviates from this dependence.

The initial current could be associated to polarization of the dipoles inside the bulk (since PET is a polar polymer) because a weak polarization mechanism is dominant at the beginning.[15] Later, the transport of charge intervenes.

From these experimental results and those given by different authors,[16–19] it can be concluded that, in a transient state and for temperatures below T_g, the current is essentially due to dipolar polarization. For temperatures above T_g, the free charge motion begins to have importance with regard to the dipolar mechanism, when temperature and field increase.

Many authors[17,20] agree that, between 70° and 100°C, α relaxation associated to T_g cannot be explained only by dipolar process but also includes space charge effect. These results are comparable with those obtained more recently by Neagu[8] on PET under similar conditions.

MODEL

Debye has shown as far back as 1920[21] that for one relaxation time dipole, the current exhibits an exponential decrease. On the other hand,

several published results[4,8,9,13,18] on a wide range of materials from polymers to ceramics have shown that transient current in an insulator never decreases exponentially. As a result, the Debye model does not give a valuable representation of real insulators. The explanation of the difference between the measured current and that calculated from the Debye model could be based on the assumption that the relaxation time was not unique but distributed according to a given law. For example, a Wagner distribution[21] leads to a t^{-m} current with $0,6 < m < 1$. Other approaches were proposed. Starting from these considerations, we assume in our calculations that the dipolar current will follow this law.

Based on this assumption, the experimental current was divided into two components: dipolar orientation current $J_d(t)$, which decays with time and follows approximately the power law $J_d(t) = A(T)t^{-m}$, and conduction current $J_c(t)$, associated to space charge transport. For comparison, two temperatures were chosen: one below the glass transition temperature T_g ($T_g = 75°C$), where the peak was not observed, and the other above T_g, where the anomalous current appears.

The two components J_c and J_d of the experimental current are shown in Figures 2(a) and 2(b) for temperatures $T = 70°C$ and $T = 100°C$ at a same electrical field 56×10^6 V/m. It can be noted from these curves that:

1. At 70°C (Figure 2(a)) the dipolar current J_d is the dominating contribution to the charging current since it appears in a large range of time from 1 to 10^2 s, then the conduction current J_c begins at 10^2 s and increases with time up to 10^4 s.
2. At 100°C (Figure 2(b)), a peak was observed at 10 min, which was not seen at 70°C. The conduction current is very important and appears rapidly, but, for the dipolar current, its contribution in the charge current appears between 1 and 10 s.

BASIC EQUATIONS

The anomalous charging current was numerically simulated using an injection process. The model consists of one kind of carrier with mobility μ, and the charge carrier is assumed to be positive. For the simulation, a one-dimensional problem was considered, in which a film of polymer is held between two metal electrodes. The lateral dimensions of the electrodes and specimen are much bigger than the thickness, d. Thus the edge effects and fringing fields can be ignored.[22]

The conduction current, $J_c(x,t)$, is:

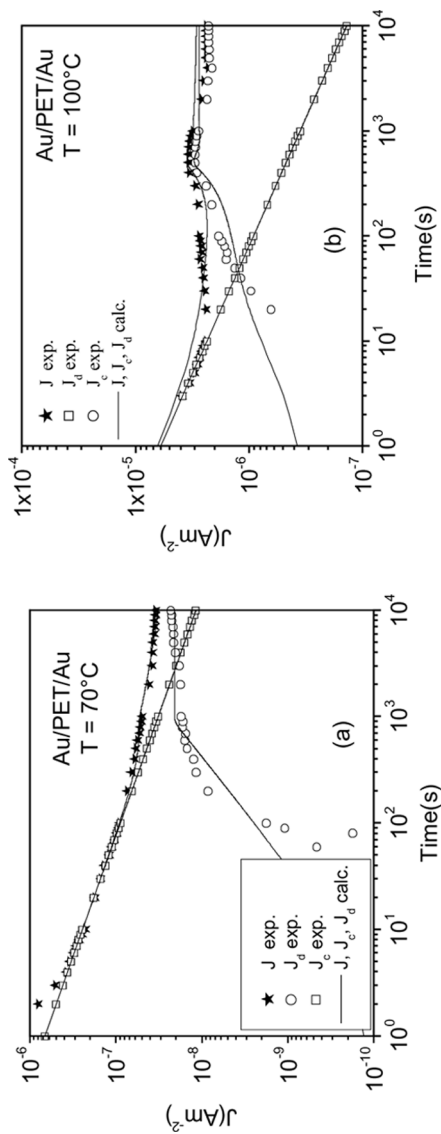$$J_c(x, t) = e\mu n(x, t)F(x, t) - eD\frac{\partial n(x, t)}{\partial x} \qquad (1)$$

Figure 2. Calculated charge current characteristics at: (a) $T = 70°C$ and (b) $T = 100°C$.

363

where $F(x,t)$ is the local electric field, e is the elementary charge, $D = \mu kT/e$ is the diffusion coefficient, k is the Boltzmann constant, T is the temperature, and n is the carrier density. The carriers drift from the anode ($x = 0$) to the cathode ($x = d$) under the local field, $F \geq 0$.

The continuity equation is expressed as follows:

$$\frac{\partial J_c(x,t)}{\partial x} = -e\frac{\partial n}{\partial t} \tag{2}$$

The internal field $F(x,t)$ is determined by Poisson's equation:

$$\varepsilon_r\varepsilon_0 \frac{\partial}{\partial x} F(x,t) = en(x,t) \tag{3}$$

where ε_r is the relative dielectric permittivity and ε_0 is the vacuum permittivity.

The circuit condition under applied voltage V is:

$$\int_0^d F(x,t)dx = V \tag{4}$$

The Schottky-type injection of carriers from the anode takes place under the enhanced anode field, giving a boundary condition. The injection current at the anode is:

$$J_c(0,t) = A_i\left\{\exp\left[\frac{e}{2kT}\sqrt{\frac{eF(0,t)}{\pi\varepsilon_r\varepsilon_0}}\right] - 1\right\} \tag{5}$$

where A_i is the injection coefficient of carriers.

The initial value of the carrier density is equal to zero ($n(x,0) = 0$).

The external total current density $J(t)$ is a function of time only and is given by:

$$J(t) = J_c(x,t) + \varepsilon_r\varepsilon_0 \frac{\partial F(x,t)}{\partial t} \tag{6}$$

The first term in the right-hand side is the particular current and the second term is the displacement current.

Therefore, the spatial integration of Equation (6) gives

$$J(t) = \frac{1}{d}\int_0^d J_c(x,t)dx + \frac{\varepsilon_r\varepsilon_0}{d}\frac{\partial}{\partial t}\int_0^d F(x,t)dx \tag{7}$$

Since the applied voltage V is constant throughout the charging process, the time derivative of Equation (4) is equal to zero.[23,24]

Equation (6) is transformed to:

$$J(t) = \frac{1}{d}\int_0^d J_c(x,t)dx \tag{8}$$

Taking into account the current due to the dipoles $J_d(t)$ and assuming that it follows from the Curie law $A(T)t^{-m}$, the total external current is written:

$$J(t) = \frac{1}{d} \int_0^d J_c(x,t)dx + A(T)t^{-m} \tag{9}$$

For the numerical treatment, the sample was divided into l equal parts in the direction of the thickness, and x was replaced by $x_k = (k-1)\Delta x$, where $\Delta x = \frac{d}{l}$, $k = 1, 2, \ldots, l+1$. In the present discussion, l was 100. The density $n(x,t)$ was approximated by the average value n_k in k-th division ($x_k \leq x \leq x_{k+1}$). The field F_k and the current J_k were the values at each division boundary ($x = x_k$). The derivatives were replaced by the difference quotients. The integration was approximated with the trapezoidal rule.

The positive charge carrier density at time $t + \Delta t$ was related to the density at time t by:

$$n_k(t + \Delta t) = n_k(t) + \Delta t \frac{\partial n_k(t)}{\partial t} \tag{10}$$

RESULTS AND DISCUSSION

The experimental and simulated current densities are compared in Figure 2 for two temperatures of $70°$ and $100°C$. The conduction and dipolar components of each current are also shown in Figure 2. It can be noted that the simulation reflects the experiment quantitatively and qualitatively. The model reproduces the current behavior in the two regions $T < T_g$ and $T > T_g$.

The calculated current did not exhibit a peak at $70°C$ because the conduction current is not important in front of the dipolar current. But at $100°C$, the conduction current starts to predominate after $50\,s$ (so that the transit of carriers is more important at $100°C$ than at $70°C$). Consequently the total current exhibits a peak.

The parameters used in the simulation for the best fit of current are reported in Table I. $A(T)$ increases with temperature from one order of magnitude, which is obvious as the dipolar current is thermally activated.

Table I. Simulation parameters at different temperatures

Temperature (°C)	$A\,(T)$	m	μ (m^2 V^{-1} s^{-1})	A_i (A/m^2)
70	6.7×10^{-7}	0.44	5×10^{-16}	10^{-10}
100	6×10^{-6}	0.41	10^{-15}	8×10^{-8}

The m exponent does not vary a lot and is to the volume $m = 0.4$ obtained by Thielen in PET.[25] The values of mobility μ are small but close to the apparent mobility obtained by other authors in their investigations on polymers.[26] The increase of injection coefficient A_i attained three decades.

Simulated Space Charge

To study the space charge, the distribution of volume charge density inside the material at $T = 100°C$ and $F_a = 40 \times 10^6\,V/m$ and its evolution in time up to $10^4\,s$ is presented in Figure 3. It can be seen that at the beginning of voltage application, space charge was very important near the injecting electrode. These homocharges, injected at the anode, slowly moved through the dielectric towards the cathode. At peak time, they reached the opposite electrode. The bulk of the insulator then remained positively charged until the end of the polarization step. The space charge density became approximately uniform and constant. These simulation
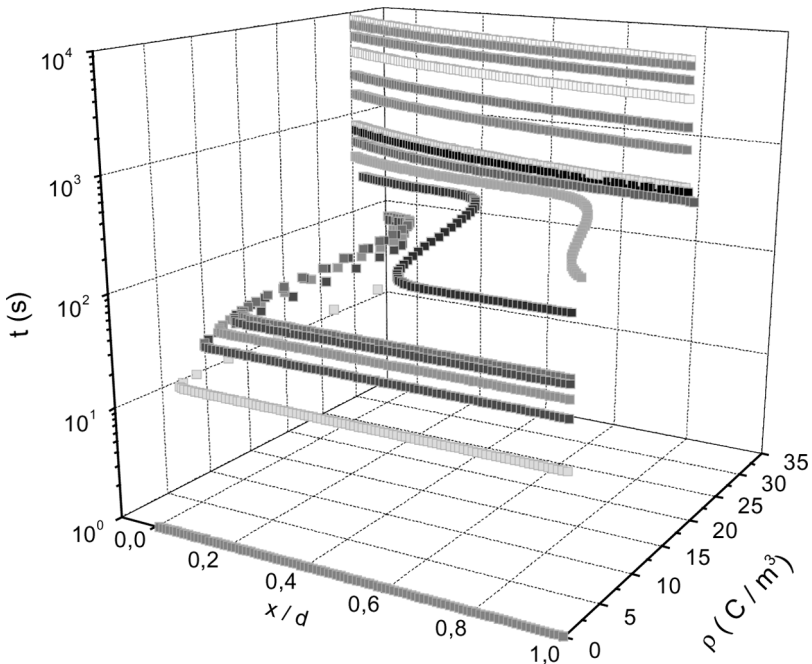

Figure 3. Evolution of space charge into Au/PET/Au sample at $T = 100°C$ and $F_a = 40 \times 10^6\,V/m$.

results are in agreement with the literature, showing the dominance of positive charges in a polymer with gold-coated electrodes.[27,28]

Electrode Effect

In a preceding work,[14] Al/PET/Al structure was studied under the same experimental conditions as those presented in this article for Au/PET/Au. The aim of this study is to compare electrical behavior of metal/PET/metal structures with different electrode metals.

   To see the effect of the nature of the electrodes on steady-state current, we presented on the same graph (Figure 4) the variation of steady current density with temperature for two types of electrodes. The curve representing $Log\ (J) = f(1000/T)$ shows that the current variation follows the Arrhenius law:

$$J = J_0 \exp\left(\frac{-E_a}{kT}\right) \tag{11}$$

where E_a is the activation energy, k is the Boltzmann constant, and T is the absolute temperature.

   We note on the one hand that in the whole range of temperatures, the current J for Al is higher than that for Au. On other hand, it should be noted that the experimental plot represents a change in the slope at the
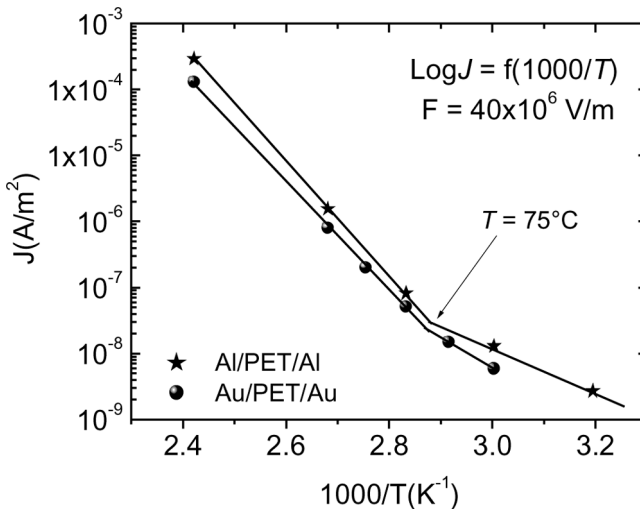

Figure 4. Temperature effect on steady-state currents in Al/PET/Al and Au/PET/Au structures.

Table II. Activation energies for the two structures

	T (°C)	
Structure	40–75	75–140
E_a (Al/PET/Al)(eV)	0.6	1.7
E_a (Au/PET/Au)(eV)	0.9	1.6

region between 60° and 80°C for Al and between 70° and 80°C for Au, showing a break point at $T = 75$°C. This defines two values of E_a above and below this temperature in each structure. The break point at the temperature of 75°C corresponds to the glass transition temperature of PET ($T_g = 75$°C).

The various activation energies given in Table II indicate an increase above T_g. These values were not affected by the nature of the electrode, which confirms that the increase of E_a at $T > T_g$ is associated with a bulk mechanism. Indeed, above T_g, the free volume increases and facilitates the transport of the charge carriers. This increase was observed with other polymers such as polyimide[29] and vinyl polychloride.[30]

The representation of $J(t)$ characteristics of Al/PET/Al in glassy and rubbery states given in Figure 5 allows one to compare features of transient current in two structures. At $T = 40$°C, normal behavior was observed, while at $T = 100$°C, a peak was observed at time $t = 500$ s.
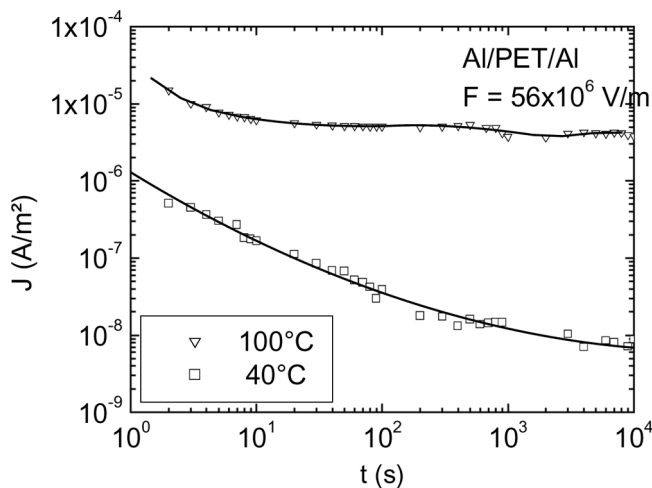
Figure 5. Charging current of Al/PET/Al structure in glassy and rubbery states.

It can be concluded that the same behavior was observed in the Au/PET/Au structure (Figure 1).

CONCLUSION

The model proposed reproduces both normal and anomalous charge currents, and it gives good agreement between the experiment and simulation. It allows one to simulate the distribution and evolution of the space charge inside the sample and to correlate it with $J(t)$ variation.

REFERENCES

[1] Wintle, H. J. (1974). Absorption currents and steady currents in polymer dielectrics. *J. Non-Cryst. Solids* **15**, 471–486.

[2] Amroun, N., M. Saidi, M. Bendaoud, and T. G. Hoang. (1993). Pressure effect on space charge in low density polyethylene (LDPE). *Mater. Chem. Phys.* **33**, 168–170.

[3] Lowell, J. (1990). Absorption and conduction currents in polymers: A unified model. *J. Phys. D Appl. Phys.* **23**, 205–210.

[4] Patsch, R. (1990). Space charge phenomena in polyethylene at high electric fields. *J. Phys. D Appl. Phys.* **23**, 1497–1505.

[5] Mizutani, T., M. Ieda, and I. B. Jordan. (1979). Anomalous transient currents in high-density polyethylene around 50–70°C. *Jpn. J. Appl. Phys.* **18**, 65–70.

[6] Adamec, V. and J. H. Calderwood. (1981). On the origin of electrical conductivity in polyethylene. *J. Phys. D* **14**, 1487–1494.

[7] Miyairi, K. and M. Ieda. (1980). Current peaks observed in polyethylene terephthalate films with linearly increasing voltage. *Jpn. J. Appl. Phys.* **19**, 1067–1071.

[8] Neagu, E. R. (2005). Combined isothermal and non-isothermal dc measurements to analyze space-charge behavior in dielectric materials. *J. Appl. Phys.* **97**(4), 044103.1–044103.9.

[9] Das Gupta, D. K. and K. Joyner. (1976). A study of absorption currents in polypropylene. *J. Phys. D Appl. Phys.* **9**, 2041–2048.

[10] Kaneko, K., Y. Suzuoki, T. Mizutani, and M. Ieda. (1990). Effect of dipoles on electrical conduction in polymers: I. Numerical calculation. *Jpn. J. Appl. Phys.* **29**, 1506–1510.

[11] Kaneko, K., Y. Suzuoki, Y. Yokota, T. Mizutani, and M. Ieda. (1992). Effect of dipoles on electrical conduction in polymers: II. Low-field conduction in polyvinylidene fluoride. *Jpn. J. Appl. Phys.* **31**, 3615–3618.

[12] Saidi-Amroun, N., H. Oubouchou, S. Berdous, M. Saidi, and M. Bendaoud. (2006). Temperature effect on transient charge and discharge currents in poly(ethylene naphthalene-2,6-dicarboxylate). *Int. J. Polym. Anal. Charact.* **11**, 159–169.

[13] Mackersie, J. W., M. J. Given, and R. A. Fouracre. (2004). Influence of gamma radiation on the properties of polyethylene naphthalate (PEN). In *Proceedings of the 2004 IEEE International Conference on Solid Dielectrics: ICSD 2004*. Piscataway, N.J.: IEEE, vol. 1, pp. 387–390.

[14] Saidi-Amroun, N., S. Berdous, M. Saidi, and M. Bendaoud. (2004). Measured and simulated transient current in polyethylene terephthalate films below and above the glass transition temperature. In *Proceedings of the 2004 IEEE International Conference on Solid Dielectrics: ICSD 2004*. Piscataway, N.J. : IEEE, vol. 1, pp. 137–140.

[15] Adamec, V. and J. H. Calderwood. (1983). The significance of dipolar mechanisms in relation to charge and discharge currents in polyethylene. *J. Phys. D Appl. Phys.* **16**, 203–211.

[16] Neagu, E., J. N. Marat-Mendes, D. K. Das-Gupta, R. M. Neagu, and R. Igreja. (1997). Analysis of thermally stimulated discharge current around glass-rubber transition temperature in polyethylene terephthalate. *J. Phys. D Appl. Phys.* **82**, 2488–2496.

[17] Gorokovatsky, Y., D. Temnov, J. N. Marat-Mendes, C. J. M. Dias, and D. K. Das-Gupta. (1998). On the nature of thermally stimulated discharge current spectra in polyethylene terephthalate. *J. Appl. Phys.* **83**, 5337–5341.

[18] Thielen, A., J. Niezette, G. Feyder, and J. Vanderschueren. (1994). Space charge due to contact effects in Al-polyethyleneterephthalate-Al systems: Modeling and study by the thermally stimulated current method. In *Proceedings of 8th International Symposium on Electrets ISE8*. Piscataway, N.J.: IEEE, pp. 319–324.

[19] Tatsumi, T., E. Ito, and R. Hayakawa. (1992). Study of the dielectric β-relaxation in poly (ethylene terephthalate) and ethylene isophthalate terephthalate copolyesters. *J. Polym. Sci. Part B Polym. Phys.* **30**, 701–706.

[20] Havriliak, S. and T. J. Shortridge. (1990). Molecular dynamics of the beta process in the polycarbonate of bisphenol-A. *Polymer* **31**, 1782–1786

[21] Bottcher, C. J. F. and P. Bordewijk. (1978). *Theory of Electric Polarization*, vol. 2. Amsterdam: Elsevier.

[22] Wintle, J. (1983). In *Engineering Dielectrics, vol. IIA, Electrical Properties of Solid Insulating Materials: Molecular Structure and Electrical Behavior*, eds. R. Bartnikas and R. M. Eichhorn. Philadelphia, Pa.: ASTM, p. 282.

[23] Kaneko, K., Y. Suzuoki, T. Mizutani, and M. Ieda. (1989). A numerical consideration of the effect of an antistatic agent on electrical conduction in polyethylene. *Jpn. J. Appl. Phys.* **28**, 1882–1886.

[24] Takai, Y., M. Kobayashi, T. Mizutani, and M. Ieda. (1988). The electronic avalanche in poly-p-xylylene thin polymer films. I: A numerical calculation. *J. Phys. D: Appl. Phys.* **21**, 1151–1158.

[25] Thielen, A., J. Niezette, G. Feyder, and J. Vanderschueren. (1994). Characterisation of polyester films used ion capacitors. I: Transient and steady-state conductivity. *J. Appl. Phys.* **76**, 4689–4695.

[26] Davies, D. K. (1972). Carrier transport in polythene. *J. Phys. D Appl. Phys.* **5**, 162–168.

[27] Le Roy, S., G. Teyssedre, C. Laurent, G. C. Montanari, and F. Palmieri. (2006). Description of charge transport in polyethylene using a fluid model

with a constant mobility: Fitting model and experiment. *J. Phys. D Appl. Phys.* **39**, 1427–1436.

[28] Chen, G., T. Y. Tay, A. E. Davis, Y. Tanaka, and T. Takada. (2001). Electrodes and charge injection in low-density polyethylene, using the pulsed electroacoustic technique. *IEEE Trans. Dielectr. Electr. Insul.* **8**, 867–873.

[29] Chang, H. K., W. M. Shen, and J. Yu. (1982). High-temperature conductivity of PI films. In *Proceedings of the 1982 IEEE Conference on Electrical Insulation and Dielectric Phenomena*. Piscataway, N.J.: IEEE, p. 108.

[30] Kosaki, M., K. Sugyama, and M. Ieda. (1971). Ionic jump distance and glass transition of polyvinyl chloride. *J. Appl. Phys.* **42**, 3388–3392.